



Mechanisms and Equilibrium Studies of Sorption of Metronidazole Using Graphene Oxide

Davoud Balarak¹, Ferdos Kord Mostafapour¹, Hossein Azarpira², Ali Joghataei^{3*}

¹Department of Environmental Health, Health Promotion Research Center, School of Public Health, Zahedan University of Medical Sciences, Zahedan, Iran.

²Saveh University of Medical Sciences, Social Determinants of Health Research Center, Saveh, Iran.

³Student Research Committee, Qom University of Medical Sciences, Qom, Iran.

Authors' contributions

This work was carried out in collaboration between all authors. All authors read and approved the final manuscript.

Article Information

DOI: 10.9734/JPRI/2017/37382

Editor(s):

(1) R. Deveswaran, Professor, M. S. Ramaiah College of Pharmacy, Bangalore, India.

Reviewers:

(1) Mihai Todica, "Babes-Bolyai" University, Romania.

(2) Julian Cruz-Olivares, Autonomous University of State of Mexico, Mexico.

Complete Peer review History: <http://www.sciencedomain.org/review-history/21832>

Original Research Article

Received 13th October 2017
Accepted 4th November 2017
Published 9th November 20YY

ABSTRACT

In this work, the removals of Metronidazole (MTZ) antibiotics onto Graphene Oxide (GO) adsorbent from aqueous solutions were studied. Batch adsorption studies were carried out at different contact time, MTZ concentrations, and temperatures. Adsorption isotherms have been modeled by Freundlich, Langmuir, Toth and Redlich-Peterson (R-P) equations. The adsorption of MTZ antibiotics was better represented by the Langmuir equation. The effect of temperature was also studied at the range between 298 and 328 K. Thermo- dynamic parameters were calculated. The positive value of enthalpy change (ΔH°) indicated the endothermic nature of the adsorption process, and the negative values of free energy change (ΔG°) were indicative of spontaneity of the adsorption process. In this work adsorption behavior of MTZ on GO sorbent was also evaluated by the data obtained from batch experiments. The positive values of ΔS° suggest the increased randomness at the sorbent-solution interface during the sorption of MTZ from the aqueous solution to the GO sorbent.

Keywords: Metronidazole; graphene oxide; pharmaceutical removal; adsorption Isotherm.

*Corresponding author: E-mail: alijoghatayi69@gmail.com;
E-mail: dbalarak2@gmail.com;

1. INTRODUCTION

Antibiotics are the most extensively used drugs to prevent or treat bacterial infections in humans, animals and plants [1,2]. Antibiotics are released into water mainly through effluents of municipal wastewater treatment plants, as well as through effluents from pharmaceutical manufacturing plants [3,4]. Antibiotics are regarded as "pseudopersistent" contaminants due to their continual considerable amount release into the environment [5,6].

Metronidazole (MNZ) with antibacterial and anti-inflammatory properties is a kind of nitroimidazole antibiotic, which is commonly used in clinical applications and widely used for the treatment of infectious diseases caused by anaerobic bacteria and protozoan's, such as *Giardia lamblia* and *Trichomonas vaginalis* [7,8]. Aside from being widely used as antibiotics for humans, MNZ is also abused as an additive in poultry and fish feed to eliminate parasites [9,10]. As a result, MNZ was accumulated in animals, fish farm water, and effluents from meat industries [11].

Many methods concerning MNZ removal from aqueous solutions have been reported, such as adsorption, photodegradation, ozonation technology, and biological methods [12-14]. The removal of pharmaceutical antibiotics by conventional water and wastewater treatment technologies is generally incomplete [15,16]. Scientists investigated the adsorption and removal of tetracycline antibiotics by several materials, including montmorillonite, rectorite, palygorskite, chitosan particles, aluminum oxide, coal humic acid, activated carbon, single-walled carbon nanotubes, and multiwalled carbon nanotubes [17,18]. However, there is still an increasing demand for the development of efficient and cost-effective treatment technologies for the removal of such pollutants [19,20].

Graphene, a novel two-dimensional carbon nanomaterials as well as being a fundamental building block for buckyballs, carbon nanotubes, and graphite has attracted a great deal of scientific interest in recent years [21]. Graphene oxide (GO), as a precursor for Graphene preparation, is always obtained through the strong oxidation of graphite by modified Hummer method [22]. Large quantities of oxygen atoms are present on the surface of the resulting GO in

the forms of epoxy, hydroxyl, and carboxyl groups. Due to its specific surface structure, it can also be used as an adsorbent. The focus on the removal of toxic elements and compounds from contaminated water/ environment by GO is emerging [23].

The objectives of this work are to evaluate the effectiveness of Oxide (GO) adsorbent for a removal of Metronidazole (MTZ) antibiotics in aqueous solution and to better understand the adsorption of MTZ onto GO. Equilibrium adsorption isotherms were measured and the experimental data were analyzed with commonly used models, namely, Langmuir, Freundlich, Toth and Redlich-Peterson isotherm equations.

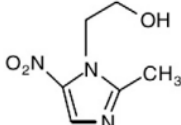
2. MATERIALS AND METHODS

All chemicals used were of analytical reagent grade and used without further purification. Graphite powder and Metronidazole was purchased from Sigma Aldrich Co. Ltd. The water used in all experiments had a resistivity higher than 18 MX cm. Also the chemical and physical characteristics of MNZ are summarized in Table 1.

GO was synthesized from graphite powder according to the modified Hummer's method. Graphite powder was added to a solution consisting of concentrated H_2SO_4 , $K_2S_2O_8$, and P_2O_5 and reacted for 4.5 h. The mixture was then diluted with 0.5 L water. Then, the mixture was filtered and washed with water for remove the residual acid. The product was dried under ambient conditions overnight. This pre-oxidized graphite was added to cold concentrated H_2SO_4 (120 mL) followed by the gradual addition of $KMnO_4$ (15 g) under stirring, and the temperature was kept below 20°C by cooling. This mixture was stirred at 35°C for 30 min and 90°C for 90 min. Afterward, the mixture was diluted with water (250 mL) and kept at 105°C for 25 min. After the resulting mixture was stirred for 2 h, 0.7 L of water and 20 mL of 30% H_2O_2 were added to end the reaction. For purification, the mixture was filtered and washed with 1:10 HCl aqueous solution and water many times. Finally, the product was further purified by dialysis for 1 week to remove the remaining metal species. Exfoliation was carried out by sonicating graphite oxide under ambient condition for 20 min. The obtained dispersion was centrifuged at 3000 rpm to remove any unexfoliated GO and then centrifuged at 16,000 rpm for 10 min to collect the residue for absorption experiment. The

residue was re-dispersed in water to obtain 0.544 mg/ml GO stock solution.

Table 1. Physical and chemical characteristics of MNZ

Molecular formula	C ₆ H ₉ N ₃ O ₃
Molecular weight (g mol ⁻¹)	171.2
Water solubility (g L ⁻¹)	9.5
pKa	2.55
Melting point (°C)	159–163
Molecular structure	

Laboratory batch studies were conducted at different adsorbent concentrations, initial adsorbate concentrations, and temperatures. The method to do adsorption consist of shaking a known volume of MTZ solutions of definite concentration containing 2 g of GO for about 120 min which were found to be a sufficient time for an equilibrium to be attained. In each experiment excluding the effect of the adsorbent dose study, 2 g of adsorbent contacted with 100 mL of adsorbate solution in a 250 mL flask at a desired temperature was shaken in a thermostat rotary shaker at constant agitation speed (200 rpm) for predetermined time intervals. After the flasks were successfully removed, centrifugation was used to separate the liquid from the solid. Centrifugation was conducted at 4000 rpm for 10 minutes. The residual MTZ were determined by high performance liquid chromatography (HPLC, Shimadzu, LC10A HPLC) equipped with a UV detector (SPD-10AV) at 318 nm. A C18 column (5 µm, 250 mm long×4.6 mm) was used, and the mobile phase was composed of a mixture of acetonitrile and water (20/80, v/v). The flow

speed was set at 1.0 mL min⁻¹, and 20 µL injections were used.

The surface area and pore volume of Graphene and Graphene Oxide were measured through N₂ adsorption at -196°C using a TRISTAR-3000 surface area and porosity analyzer (Micromeritics).

3. RESULTS AND DISCUSSION

N₂ adsorption shows that graphite has a BET surface area and pore volume of 19.5 m²/g and 0.087 cm³/g, respectively. After oxidation, GO has a surface area of 28 m²/g and pore volume of 0.097 cm³/g. Fig. 1 shows plots of XRD for graphite and graphite oxide. In the pattern of GO, the peak at 2θ=27.2° was no longer detected and a new broader peak appeared at 2θ=10.4°, demonstrated that the graphene structure with new oxygen containing groups was formed successfully by the strong oxidation reaction on the graphite.

3.1 Influence of Contact Time and Initial MTZ Concentration

The influence of contact time on MNZ sorption by GO was studied (Fig. 2). The results show that adsorption capacity (q_e) increased with an increase contact time for all concentrations and sorption of MNZ is rapid, and more than half the amount of MNZ is remove in the first 30 min; thereafter, the sorption rate decreases gradually and reaches the equilibrium in 75 min. Thus, optimum contact time of 75 min was selected for further studies. The MNZ adsorption rate is high at the beginning of the experiment because initially the adsorption sites are more available and MNZ ions are easily adsorbed on these sites [24,25].

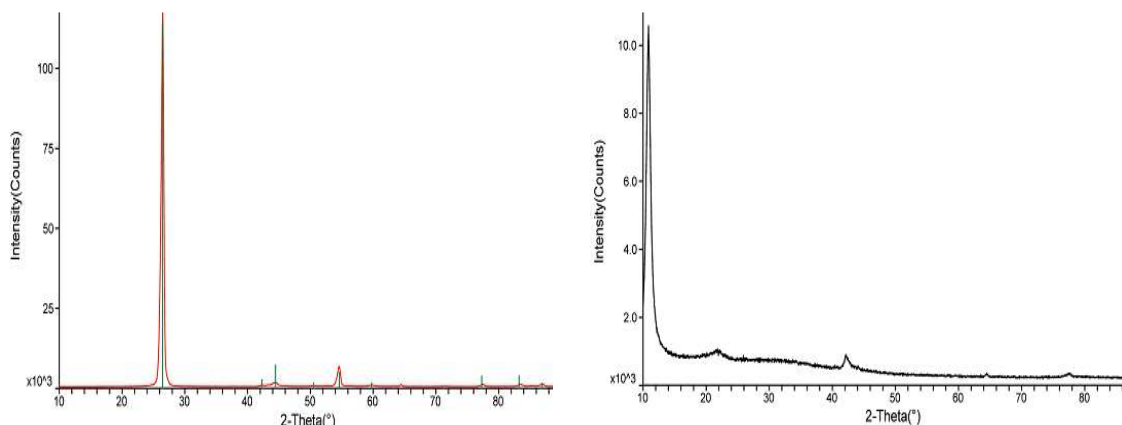


Fig. 1. XRD of graphite and graphite oxide

3.2 Influence of Stirring Rate

Stirring rate influences the distribution of the solute in the bulk solution and formation of the external boundary layer [26]. The influence of stirring rate on the removal of MNZ by the GO sorbent was examined by changing the stirring rate between 0 (without stirring) to 300 rpm, while keeping all other experimental conditions constant. It was observed (as in Fig. 3) that with a fixed stirring time, an increase in the stirring rate up to 300 rpm caused an increase in the sorbents capacity and decreased equilibrium liquid-phase concentrations (C_e) which leveled off at a higher speed. Thus, the stirring rate of 250 rpm ensured that the

solid was completely and homogenously suspended in the solution, and hence, the further increase in the stirring speed had no significant effect on the sorption capacity [27,28]. So, the stirring rate of 250 rpm was chosen as the optimum speed for all the sorption experiments.

3.3 Adsorption Isotherms

Study of adsorption equilibrium isotherms is an important step in investigating adsorption processes since it makes it possible to identify the relationship between the amounts of MTZ adsorbed and in solution, after equilibrium is reached.

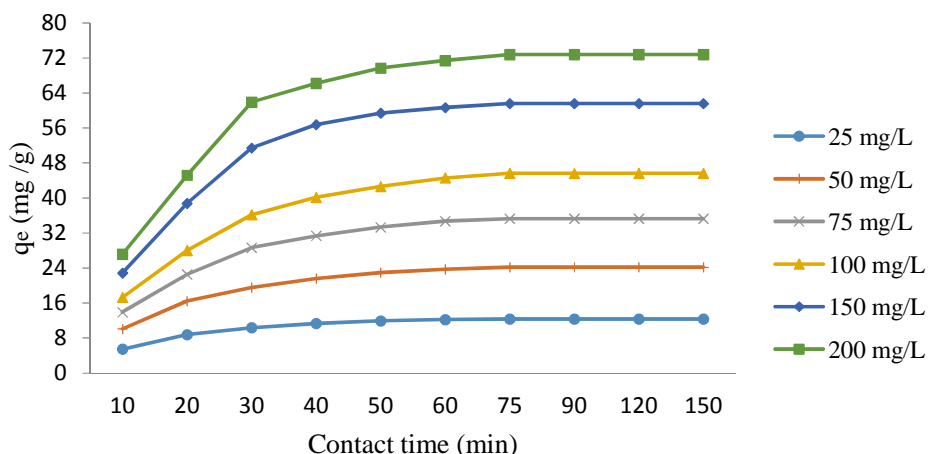


Fig. 2. Effect of contact time and initial MTZ concentration (pH = 7, dose: 2 g/L and temp 30 °C and stirring rate 200 rpm)

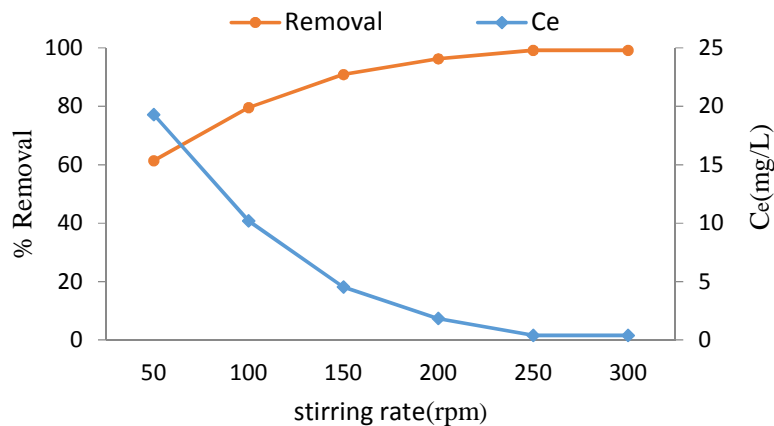


Fig. 3. Effect of adsorbent dose (Contact time = 75 min, pH = 7, Con: 50 mg/L and temp 30 °C and dose: 2 g/L)

Although linear regression has been widely used to estimate the isotherm parameters, the way the linearization of non-linear isotherm expressions is done may lead to different changes in error distributions and violation of the normality suppositions of the least-square method, which makes linearization an inappropriate approach [29]. A computer program has been used for the estimation of coefficients based on non-linear optimization technique. The value of the mean absolute percentage error [30,31].

The following equation has been selected as a test criterion for the fit of the correlation and used to estimate the isotherm parameters of Langmuir, Freundlich, Toth and Redlich-Peterson models for a better understanding of the interactions between adsorbent materials and MTZ adsorbate [32].

$$\% \text{ Error} = \frac{q_e(\text{experimental}) - q_e(\text{predicted})}{q_e(\text{experimental})} \times 100 \quad (1)$$

3.4 Langmuir Adsorption Isotherm

The Langmuir isotherm is based on the assumption that adsorption takes place at specific homogeneous sites within the adsorbent and there is no significant interaction among adsorbed species. The adsorbent is saturated after one layer of adsorbed molecules is formed on the adsorbent surface. The Langmuir isotherm is represented by Equation 2 [33,34]:

$$q_e = \frac{qbC_e}{1+bC_e} \quad (2)$$

Where q is the monolayer capacity of the adsorbent (mg/g) and b is the Langmuir adsorption constant related to the energy of adsorption (L/mg). In this work, the Langmuir isotherm best fits the experimental data for lower values of C_e , indicating that initially the adsorption process occurs as a monolayer phenomenon. However, this mechanism does not persist under higher concentration ranges and in these cases the adsorption seems to be a multilayer process.

3.5 Freundlich Adsorption Isotherm

The Freundlich isotherm model takes multilayer and heterogeneous adsorption into account. The Freundlich isotherm model is given by Equation 3 [35,36]:

$$q_e = K_F C_e^{\frac{1}{n}} \quad (3)$$

Where K_F (L/mg) and n are Freundlich isotherm constants, indicative of the saturation capacity and intensity of adsorption. It is well known that $1/n$ values between 0.1 and 1 indicate a favorable adsorption. As shown in Table 2, $1/n$ values lower than unity that implies stronger interaction between MTZ adsorbent and GO.

3.6 Redlich-Peterson Isotherm

Redlich-Peterson is an empirical equation, with three parameters, which is capable of representing adsorption equilibrium over a wide concentration range. This equation has the form [37,38]:

$$q_e = \frac{\alpha_R C_e}{1 + b_R C_e^\beta} \quad (4)$$

Where α_R (L/mg), b_R (L/mg) and β are the isotherm constants. This equation is an empirical one and reduces to Henry's law, Freundlich or Langmuir under appropriate condition. The Redlich-Peterson model incorporates the characteristics of Langmuir and Freundlich isotherms into a single equation. Two limiting behaviors exist, i.e., Langmuir form for β equal to 1 and Henry's law form for β equal to 0. The β values are far from unity in adsorption of MTZ (Table 2). This means that the data can't preferably be fitted with the Langmuir model for these GO.

3.7 Toth Isotherm

Toth has modified the Langmuir equation to reduce the error between experimental data and predicted values of equilibrium adsorption data. The application of his equation is best suited to multilayer adsorption similar to BET isotherms, which is a special type of Langmuir isotherm and has very restrictive validity. The Toth isotherm model is given by Equation 5 [39,40]:

$$q_e = \frac{q_t K_T C_e}{[1 + (K_T C_e)^{n_T}]^{\frac{1}{n_T}}} \quad (5)$$

Where q_e is the adsorbed amount at equilibrium (mg/g), C_e the equilibrium concentration of the adsorbate (mg/L), q_t the Toth maximum adsorption capacity (mg/g), K_T the Toth equilibrium constant, and n_T is the Toth model exponent. The parameters obtained for Toth isotherms are shown in Table 2 and were used to identify the models that best fit the experimental data.

In general, the data obtained from the adsorption isotherms experiments appeared to be well represented by all theoretical models tested. It was found that the Langmuir isotherm for MTZ gave an excellent overall fit. Among the parameter models investigated in this study, the

better known Freundlich isotherm gave the worst fitting for MTZ with (% error=14.3), if compared to the rest of models. Whereas, the rarely used Redlich-Peterson isotherm gave much better fitting for MTZ with (% error=0.978) only. The isotherms plot is shown in Fig. 4 a-d.

Table 2. The adsorption isotherms constants for the removal MTZ onto GO

Langmuir				Freundlich			
q_e	b	R^2	% Error	K_F	$1/n$	R^2	% Error
89.7	0.39	0.998	5.3	12.2	0.41	0.917	14.3
Toth				Redlich-Peterson			
q_T	K_T	R^2	% Error	α_R	b_R	R^2	% Error
98.4	0.47	0.937	3.2	31.8	0.51	7.6	0.976

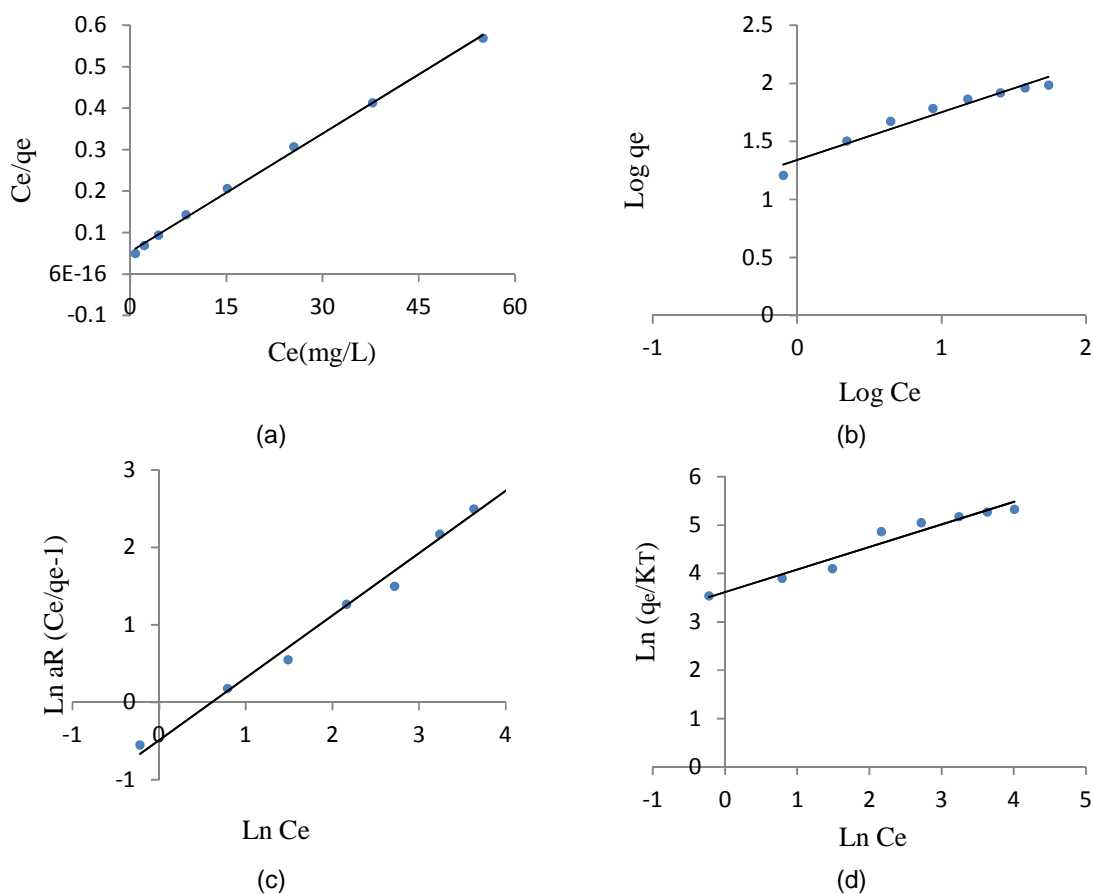


Fig. 4. isotherm models for the adsorption of MTZ adsorption onto GO, (a) Langmuir (b) Freundlich (C) Redlich-Peterson (d) Toth

Table 3. Thermodynamic parameters for sorption of MTZ on GO

T (K)	q_e (mg/g)	K_C	ΔG° (kJ/mol)	ΔH° (kJ/mol)	ΔS° (J/mol K)
298	75.22	1.15	- 0.346		
308	80.46	1.28	- 0.632	32.86	7.93
318	86.38	1.44	- 0.964		
328	84.1	1.62	- 1.315		

3.8 Thermodynamic of the Sorption of MTZ on GO

Thermodynamic of the sorption of MTZ by the GO sorbent was studied by varying the temperature in the range of 298–318 K under other optimized conditions (Table 3). As it is observed, an increase in the temperature from 298 to 318 K caused an increase in the MTZ removal by GO sorbent. The thermodynamic parameters including the Gibbs free energy (ΔG°), the enthalpy (ΔH°) and the entropy (ΔS°) were determined using the Equation 6-8 [41-43]:

$$K_c = \frac{q_e}{C_e} \quad (6)$$

$$\Delta G^\circ = -RT \ln K_c \quad (7)$$

$$\ln K_c = \frac{\Delta S^\circ}{R} - \frac{\Delta H^\circ}{RT} \quad (8)$$

Where C_e is the equilibrium concentration (mg/L) of the MTZ solution, K_c (L/g) is the equilibrium constant, q_e is the equilibrium adsorption capacity (mg/g), ΔG° is the Gibbs free energy change in sorption (kJ/mol), ΔS° is the entropy change in sorption [kJ/(mol K)], ΔH° is the change in enthalpy in sorption (kJ/mol), T is the absolute temperature (K) and R is the universal gas constant [8.314 J/(mol K)]. The calculated thermodynamic parameters are also provided in Table 3. As it can be seen, the value of K_c increased with an increase in the temperature from 298 to 328 K, favoring the sorption of MTZ. The negative values of ΔG° and the positive value of ΔH° at different temperatures indicate that the sorption of MTZ is spontaneous and endothermic, respectively. The positive values of ΔS° suggest the increased randomness at the sorbent–solution interface during the sorption of MTZ from the aqueous solution to the GO sorbent [44-46].

4. CONCLUSION

Adsorption and thermodynamic studies were accomplished for the MTZ removal using GO. The results show that adsorption processes are significantly affected by temperature. The thermodynamic studies indicated that the adsorption of MTZ onto GO is spontaneous and endothermic in nature. Overall, the results suggested that the GO is an efficient adsorbent for application in treating Metronidazole existing in pharmaceuticals wastewater streams.

CONSENT

It is not applicable.

ETHICAL APPROVAL

It is not applicable.

COMPETING INTERESTS

Authors have declared that no competing interests exist.

REFERENCES

1. Balarak D, Mostafapour FK, Joghtaei A. Thermodynamic analysis for adsorption of amoxicillin onto magnetic carbon nanotubes. *British Journal of Pharmaceutical Research*. 2017;16(6):1-10.
2. Peng X, Hu F, Dai H, Xiong Q. Study of the adsorption mechanism of ciprofloxacin antibiotics onto graphitic ordered mesoporous carbons. *Journal of the Taiwan Institute of Chemical Engineers*. 2016;8:1–10.
3. Amini M, Khanavi M, Shafiee A. Simple high-performance liquid chromatographic method for determination of ciprofloxacin in human plasma. *Iranian Journal of Pharmaceutical Research*. 2004;2:99-101.
4. Carabineiro A, Thavorn-Amornsri T, Pereira F, Figueiredo L. Adsorption of ciprofloxacin on surface modified carbon materials. *Water Res*. 2011;45:4583-91.
5. Ibezim EC, Ofoefule SI, Ejeahalaka N, Orisakwe E. *In vitro* adsorption of ciprofloxacin on activated charcoal and talc. *Am J Ther*. 1999;6(4):199-201.
6. Ghauch A, Tuqan A, Assi HA. Elimination of amoxicillin and Ampicillin by micro scale and nano scale iron particles. *Environ Pollut*. 2009;157:1626–1635.
7. Balarak D, Azarpira H. Photocatalytic degradation of Sulfamethoxazole in water: investigation of the effect of operational parameters. *International Journal of Chem Tech Research*. 2016;9(12):731-8.
8. Balarak D, Mostafapour FK, Joghataei A. Experimental and kinetic studies on penicillin g adsorption by lemna minor. *British Journal of Pharmaceutical Research*. 2016;9(5):1-10.
9. Balarak D, Mahdavi Y, Maleki A, Daraei H and Sadeghi S. Studies on the removal of

- amoxicillin by single walled carbon nanotubes. British Journal of Pharmaceutical Research. 2016;10(4):1-9.
10. Balarak D, Mahdavi Y, Mostafapour FK. Application of alumina-coated carbon nanotubes in removal of tetracycline from aqueous solution. British Journal of Pharmaceutical Research. 2016;12(1):1-11.
 11. Alexy R, Kumpel T, Kummerer K. Assessment of degradation of 18 antibiotics in the closed bottle test. Chemosphere. 2004;57:505–512.
 12. Balarak D, Mostafapour FK. Canola Residual as a biosorbent for antibiotic metronidazole removal. The Pharmaceutical and Chemical Journal. 2016;3(2):12-17.
 13. Malakootian M, Balarak D, Mahdavi Y, Sadeghi SH, Amirmahani N. Removal of antibiotics from wastewater by *Azolla filiculoides*: Kinetic and equilibrium studies. International Journal of Analytical, Pharmaceutical and Biomedical Sciences. 2015;4(7):105-113.
 14. Aksu Z, Tunc O. Application of biosorption for *Penicillin G* removal: Comparison with activated carbon. Process Biochemistry. 2005;40(2):831-47.
 15. Ji L, Chen W, Duan L, Zhu D. Mechanisms for strong adsorption of tetracycline to carbon nanotubes: A comparative study using activated carbon and graphite as adsorbents. Environ. Sci. Technol. 2009;43(7):2322–27.
 16. Choi KJ, Kim SG, Kim SH. Removal of antibiotics by coagulation and granular activated carbon filtration. J. Hazard. Mater. 2008;151:38–43.
 17. Zhang W, He G, Gao P, Chen G. Development and characterization of composite nanofiltration membranes and their application in concentration of antibiotics. Sep Purif Technol. 2003;30:27–35.
 18. Balarak D, Azarpira H. Rice husk as a biosorbent for antibiotic metronidazole removal: Isotherm studies and model validation. International Journal of Chem Tech Research. 2016;9(7):566-573.
 19. Yu F, Li Y, Han S, Jie Ma J. Adsorptive removal of antibiotics from aqueous solution using carbon materials. Chemosphere. 2016;153:365–385.
 20. Zhang L, Song X, Liu X, Yang L, Pan F. Studies on the removal of tetracycline by multi-walled carbon nanotubes. Chem. Eng. J. 2011;178:26–33.
 21. Sitko R, Turek E, Zawisza B, Malicka E, Talik E. Adsorption of divalent metal ions from aqueous solutions using graphene oxide. Dalton Transactions. 2013;16:1-9.
 22. Sharma P, Das MR. Removal of a cationic dye from aqueous solution using graphene oxide nanosheets: Investigation of adsorption parameters. J. Chem. Eng. Data. 2013;58(1):151–8.
 23. Fan L, Luo C, Li X, Lu F, Qiu H, Sun M. Fabrication of novel magnetic chitosan grafted with graphene oxide to enhance adsorption properties for methyl blue. Journal of Hazardous Materials. 2012; 215-216:272-9.
 24. Liu H, Liu W, Zhang J, Zhang C, Ren L, Li Y. Removal of cephalexin from aqueous solution by original and Cu(II)/Fe(III) impregnated activated carbons developed from lotus stalks kinetics and equilibrium studies. J Hazard Mater. 2011;185:1528–35.
 25. Putra EK, Pranowoa R, Sunarsob J, Indraswatia N, Ismadjia S. Performance of activated carbon and bentonite for adsorption of amoxicillin from wastewater: Mechanisms, isotherms and kinetics. Water Res. 2009;43:2419-2430.
 26. Li Q, Sun L, Zhang Y, Qian Y, Zhai J. Characteristics of equilibrium, kinetics studies for adsorption of Hg(II) and Cr(VI) by polyaniline/humic acid composite. Desalination. 2011;266:188–194.
 27. Gupta RK, Singh RA, Dubey SS. Removal of mercury ions from aqueous solutions by composite of polyaniline with polystyrene, Sep. Purif. Technol. 2004;38:225–232.
 28. Zazouli MA, Mahvi AH, Mahdavi Y, Balarak D. Isothermic and kinetic modeling of fluoride removal from water by means of the natural biosorbents sorghum and canola. Fluoride. 2015;48(1):15-22.
 29. Liu Z, Xie H, Zhang J, Zhang C. Sorption removal of cephalexin by HNO₃ and H₂O₂ oxidized activated carbons. Sci China Chem. 2012;55:1959–67.
 30. Balarak D, Mostafapour FK. Biosorption of acid green 25 from textile dye effluent using barley husk. International Journal of Advanced Biotechnology and Research. 2017;8(1):128-135.
 31. Azarpira H, Mahdavi Y, Khaleghi O, Balarak D. Thermodynamic studies on the removal of metronidazole antibiotic by

- multi-walled carbon nanotubes. *Der Pharmacia Lettre*. 2016;8(11):107-13.
32. Balarak D, Mostafapour FK, Bazrafshan E, Saleh TA. Studies on the adsorption of amoxicillin on multi-wall carbon nanotubes. *Water Science and Technology*. 2017; 75(7):14-20.
33. Balarak D, Jaafari J, Hassani G, Mahdavi Y, Tyagi I, Agarwal S, Gupta VK. The use of low-cost adsorbent (Canola residues) for the adsorption of methylene blue from aqueous solution: Isotherm, kinetic and thermodynamic studies. *Colloids and Interface Science Communications. Colloids and Interface Science Communications*. 2015;7:16–19.
34. Peterson JW, Petrasky LJ, Seymour MD, Burkhardt RS, Schuilinga AB. Adsorption and breakdown of penicillin antibiotic in the presence of titanium oxide nanoparticles in water. *Chemosphere*. 2012;87(8):911–7.
35. Balarak D, Mahdavi Y, Bazrafshan E, Mahvi AH, Esfandyari Y. Adsorption of fluoride from aqueous solutions by carbon nanotubes: Determination of equilibrium, kinetic and thermodynamic parameters. *Fluoride*. 2016;49(1):35-42.
36. Zazouli MA, Mahvi AH, Dobaradaran S, Barafrahshtehpour M, Mahdavi Y, Balarak D. Adsorption of fluoride from aqueous solution by modified *Azolla filiculoides*. *Fluoride*. 2014;47(4):349-58.
37. Gao J, Pedersen JA. Adsorption of sulfonamide antimicrobial agents to clay minerals. *Environ. Sci. Technol*. 2005; 39(24):9509-16.
38. Balarak D, Mostafapour FK, Akbari H, Joghtaei A. Adsorption of amoxicillin antibiotic from pharmaceutical wastewater by activated carbon prepared from *Azolla filiculoides*. *British Journal of Pharmaceutical Research*. 2017;18(3):1-11.
39. Balarak D, Joghataei A, Azarpira H, Mostafapour FK. Biosorption of amoxicillin from contaminated water onto palm bark biomass. *International Journal of Life Science and Pharma Research*. 2017; 7(1):9-16.
40. Balarak D, Mahdavi Y, Bazrafshan E, Mahvi AH. Kinetic, isotherms and thermodynamic modeling for adsorption of acid blue 92 from aqueous solution by modified *Azolla filiculoides*. *Fresenius Environmental Bulletin*. 2016;25(5):1321-30.
41. Dutta M, Dutta NN, Bhattachary KG. Aqueous phase adsorption of certain beta-lactam antibiotics onto polymeric resins and activated carbon. *Separation and Purification Technology*. 1999;16(3);213-24.
42. Balarak D, Mostafapour FK. Batch equilibrium, kinetics and thermodynamics study of sulfamethoxazole antibiotics onto *Azolla filiculoides* as a novel biosorbent. *British Journal of Pharmaceutical Research*. 2016;13(2):1-14.
43. Balarak D, Mostafapour FK, Azarpira H. Adsorption kinetics and equilibrium of ciprofloxacin from aqueous solutions using *Corylus avellana* (Hazel nut) activated carbon. *British Journal of Pharmaceutical Research*. 2016;13(3):1-14.
44. Agarwal S, Tyagi I, Gupta VK, Dehghani MH, Jaafari J, Balarak D. Rapid removal of noxious nickel (II) using novel gamma-alumina nanoparticles and multiwalled carbon nanotubes: Kinetic and isotherm studies. *Journal of Molecular Liquids*. 2016;224:618-623
45. Balarak D, Mostafapour FK, Azarpira H. Biosorption of reactive blue 19 dye using lemna minor: Equilibrium, kinetic and thermodynamic studies. *Bioscience Biotechnology Research Communications*. 2016;9(3):558-566.
46. Balarak D, Bazrafshan E, Mahdavi Y, Lee SM. Kinetic, isotherms and thermodynamic studies in the removal of 2-chlorophenol from aqueous solution using modified rice straw. *Desalination and Water Treatment*. 2017;63:203-211.

© 2017 Balarak et al.; This is an Open Access article distributed under the terms of the Creative Commons Attribution License (<http://creativecommons.org/licenses/by/4.0>), which permits unrestricted use, distribution, and reproduction in any medium, provided the original work is properly cited.

Peer-review history:

The peer review history for this paper can be accessed here:
<http://sciencedomain.org/review-history/21832>